RESEARCH OF ALUMINUM HOOD CONSTRUCTION FOR PEDESTRIAN PROTECTION BY OPTIMIZATION CAE

Osamu, Ito
Kazutada, Sasaki
Honda R&D Co., Ltd. Automobile R&D Center
Japan

Paper Number 17-0246

ABSTRACT

According to Japanese traffic accident statistics, the number of overall casualties on a downward trend but still more than a 1000 fatalities of pedestrian still occurred every year. Therefore, it is important that automobile manufacturers research the safety of vehicles for pedestrians. Especially, it is necessary to study bonnet hood construction that the pedestrian's head impacts reduce head injury as cause of fatality. On the other hand, body construction of vehicle must consider weight reduction so as to reduce the CO2 emissions. For that reason, automobile manufacturers have increased the use of aluminum for bonnet hood. It is known that longer crash strokes are needed for pedestrian protection if aluminum hood is used compared with steel hood. It is because that energy absorption characteristic is inferior in aluminum on account of low inertia weight and low stiffness. Accordingly, longer clearances under the hood are needed and restrictions of layout increase if the aluminum hood is adopted. To combine pedestrian protection and weight reduction has high design difficulty for automobile manufacture. The authors studied aluminum hood construction that can reduce pedestrian crash stroke convent conserving pedestrian protection performance in order to reduce restrictions of layout.

Since the pedestrian's head may impact to any location on the hood, several evaluation points are needed for validating the pedestrian protection performance. In order to design validated point easily, independent construction is desirable. In this research, emboss construction was adopted for the hood, in order to lower the stiffness response for each evaluation point. Furthermore, a CAD parameter model of this emboss hood was created, and optimization CAE was combined. Injury values and strokes were evaluated by the optimization CAE. Convergence of solution takes much time from the several evaluation points and variables if optimization is performed. Then, at the beginning, 30 designs were created with uniform random number. Secondly, they were calculated so that it could look down at overall performance in order to find the most severe evaluation point, which it is difficult to meet the HIC requirement. Thirdly, for the most severe evaluation point, optimization CAE was performed so that stroke could be minimized. Lastly, the optimized shape in the severe evaluation point was validated whether performance of other validation points were also improved.

Because of optimization CAE, the head impactor stroke was reduced 6% compared to the conventional aluminum hood. Moreover, HIC value of all validation points was below target value.

As a result of analyzing design variable contribution, various factor existed for HIC and stroke. Sheet thickness and gap between hood frame and skin had influence on both stroke and HIC. In addition, the array pattern had influence on only HIC. After deceleration of the impactor was determined by hood gap and sheet thickness from 0msec to 4msec, it was determined by emboss pattern after 4msec. However, in order to apply this research to vehicle development, it is necessary to review the stamping manufacturability of aluminum and to re-set design variable as probable realistic range.

The authors studied aluminum hood construction where both low HIC and low stroke were realizable. This research could contribute to improvement in both pedestrian protection performance and weight reduction.

INTRODUCTION

According to Japanese traffic accident statistics, 34.9% of all the fatal accident is pedestrian accident [1]. In order to reduce pedestrian fatal accident, regulation and assesment tests are performed to validate pedestrian protection preformance all over the wrold. The test validating pedestrian head protection performance is evaluated by HIC (Head Injury Criterion) using a head impactor [Equation 1]. As test area agree with WAD (Wrap Around Distance), parts of vehicle front side are evaluated [2]. Because most of test area is near the bonnet hood, it is important to study hood construction to improve head protection performance [Figure 1].

Automobile manufacture which adopts not steel but aluminum for bonnet hood is increasing in recent years. Certain crash strokes are needed for pedestrian protection in case aluminum hood is used compared with steel hood. It is because that energy absorption characteristic is inferior in aluminum on account of low inertia weight and low stiffness. Therefore, longer clearances under hood are needed and restrictions of layout increase if aluminum hood is adopted.

In past study, Ikeda et al.[3] developed a hood structure that reduced pedestrian crash stroke rather than conventional hood while maintaining HIC value. However, the structure could not reduce crash stroke when HIC value is 1000 or less. Weiss et al.[4] deviced hood design method by geometry based optimization CAE taking pedestrian protection into considaration. The method could search most efficient shape regarding concept design. The authors studied hood structure to reduce crash stroke also in case of low HIC value appling the method which Weiss et al. determined.

$$HIC = \left[(t_2 - t_1)\left[\frac{1}{(t_2 - t_1)}\int_{t1}^{t2} G(t)dt\right]^{2.5}\right]_{MAX}$$

(Equation 1)

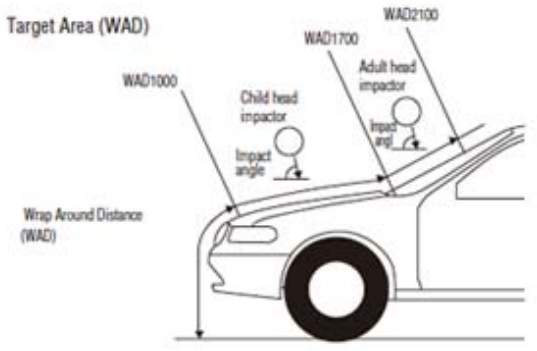

Figure 1. Wrap Around Distance. (http://www.nasva.go.jp)

METHODOLOGY

Ideal Characteristic of HIC650

According to Equation 1, there are many waveforms to be a certain HIC. Okamoto et al. [5] led the acceleration equation to minimize stroke in the same HIC [Equation 2]. Ideal G-t waveform become Figure 2 when 650 is substitued for HIC in this equation. Waveform which raises initial G and lowers the latter G appropriately has good efficency of stroke as this figure. However, this waveform can not be realized acctually because Figure 2 has inifint deceleration at 0msec. Therefore, the authors defined the target waveform such as initial G is 120G and the lattar G is 60G [Figure 3].

$$\int G(t) = HIC^{0.4} \cdot t^{0.6}$$

$$G(t) = 0.6 \cdot HIC^{0.4} \cdot t^{-0.4} \qquad \textbf{(Equation 2)}$$

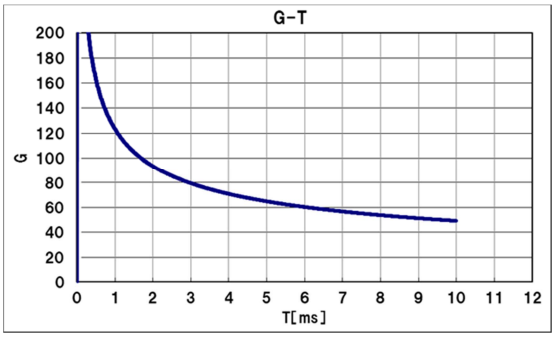

Figure 2. Ideal Characteristic Curve of HIC650.

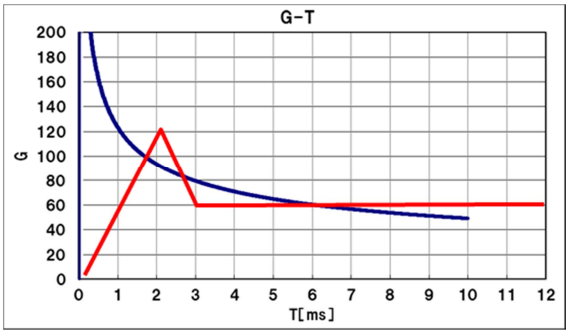

Figure 3. Target Curve of HIC650. (Red curve)

Control of Deceleration

Equation 3 and Equation 4 are from the energy conservation law and momentum conservation law. The meaning of each character shows Figure 4. In addition, Equation 5 is from both equations. This equation shows that deceleration is governed by hood stiffness and mass. It is necessary to control the waveform such that initial G can be raised and the latter G can be lowered to realize the target waveform in Figure 3.

$$\frac{1}{2}mV_0{}^2 = \frac{1}{2}(m + M_e)V^2 + mas \qquad \textbf{(Equation 3)}$$

$$mV_0 = (m + M_e)V \qquad \textbf{(Equation 4)}$$

$$a = \frac{1}{2}mV_0^2 \cdot \frac{1}{s} \cdot \frac{M_e}{m + M_e}$$

$$a = \frac{1}{2}mV_0^2 \cdot K(t) \cdot M(t) \qquad \textbf{(Equation 5)}$$

where,
K(t):Hood Stiffness
M(t):Impactor and Hood Effective Mass

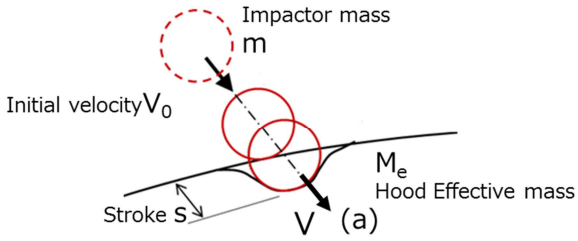

Figure 4. Meaning of Each Character.

Concept of Hood Construction

Effective-mass Aluminum hood has low effective mass due to low mass density. Holes of conventional aluminum hoods were filled in order to add effective mass in this study [Figure 5].

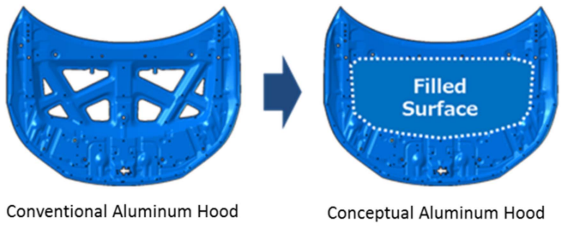

Figure 5. Hood construction with filled surface

Hood-Stiffness Because head impactor moves with the hood when the crash time advances, the effective mass continues increasing. Therefore, it is necessary to control hood stiffness in order to vary deceleration at initial and the latter time such as target waveform. On the other hand, pedestrian protection test evaluates many validation points on hood. For this reason, it is desirable to be able to control stiffness at every validation point. Consequently, the authors set independent pattern structure on the hood. After we create appropriate shapes for independent elements, each characteristic was validated by comparison investigation [Table 1]. The items are geometrical load transfer, amount of design variable, productivity and layout restriction. If there are many ridge lines, concern will increase regarding manufacturability and design restrictions. Even if the item of reduced ridgeline does not have surface at the top, load transfer efficiency will be low. As results, most appropriate independent shape was determined to frustum. The authors call it emboss structure [Figure 6].

Table 1.
Comparison of independent shape

	Load transfer	Amount of design variable	Productivity	Layout
	○	○	×	×
	○	○	×	×
	△	△	△	△
	×	×	○	○
	○	○	△	○

Figure 6. Hood concept for pedestrian protection

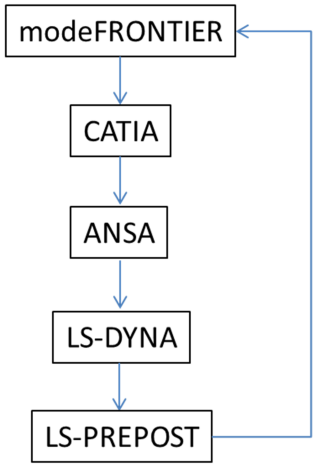

Figure 7. Schematic diagram of optimization CAE

Optimization CAE system

CAE-work-flow In order to reach concrete structure to be able to reduce crash stroke from devised concept shape, optimization CAE was performed. modeFRONTIER was used for optimization CAE software. CATIA was used for modification of aluminum hood shape. ANSA was used for creating mesh. LS-DYNA was used as FEM solver. LS-PrePost was used for post results process. Calculation work flow is in Figure 7 using optimization CAE system.

Design-variables Table 2 shows the design variables set in modeFRONTIER. The authors considered that numbers of emboss and distance during emboss may affect to the stiffness of hood. In order to avoid to increase design variables, dependent variable was used for numbers of emboss defined by emboss distance and diameter [Equation 6, 7]. Figure 8 shows relationships between arithmetic expressions and emboss shape. This diameter and distance were used only when determining numbers of emboss. As the authors consider that gap between hood skin and hood frame may has effect to increase effective

Table 2.
Design Variables for optimization

ID	Parameters	Name	Lwr	Upr	Level	Width
1	Vertical emboss distance	CH	5	50	10	5
2	Horizontal emboss distance	CL	5	60	12	5
3	Representative diameter	D	45	95	11	5
4	Gap between hood skin and frame	Offset	0	5	6	1
5～8	4 Angles of corner emboss	Angle_A	45	85	9	5
		Angle_B	45	85	9	5
		Angle_C	45	85	9	5
		Angle_D	45	85	9	5
9～12	4 Diameters of corner emboss	Dia_A	30	100	15	5
		Dia_B	30	100	15	5
		Dia_C	30	100	15	5
		Dia_D	30	100	15	5
13	Array patern	SORT	0	1	2	1
14	Frame thickness	T_FRAME	0.8	1.1	4	0.1
15	Skin thickness	T_SKIN	1	1.2	3	0.1

mass, adding to design variables [Figure 9]. Because the authors also thought each emboss angle and each diameter may has effect, adding to design variables. However, design variables have huge numbers if each emboss angle and each diameter were set to design variable. Then design variables was reduced by linear interpolation during 4 embosses at the corner such as Figure 10. In addition, emboss pattern was set to 2 patterns such as Figure 11. The design variable was defined by numbers that crosscut pattern was 0 and alternate pattern was 1. Finally, thickness of hood skin and frame were added to design variables.

$$\mathrm{NH} = \mathrm{floor}((450)/(2 * \mathrm{R} + \mathrm{D} + \mathrm{CH}) - 1)$$
(Equation 6)

$$\mathrm{NL} = \mathrm{floor}((1200)/(2 * \mathrm{R} + \mathrm{D} + \mathrm{CL}) - 1)$$
(Equation 7)

where,
NH : Number of vertical emboss (3≤NH≤6)
NL : Number of horizontal emboss (9≤NL≤19)
CH : Representative emboss distance (Row)
CL : Representative emboss distance (Column)
D : Representative diameter
R : Fixed by R5
floor: Truncation of digits

Vehicle-model Mass production vehicle of sedan type with aluminum hood was used for vehicle CAE model (Figure 12). After marking all validation points on the vehicle defined by Euro-NCAP, the authors extracted 9 validation points in order to evaluate comprehensively. Then these extracted points were determined as validation points for CAE model [Figure 13]. Target HIC were set to 650 and 1000 based on evaluation method of Euro-NCAP. In general, CAE result has some errors depending on simulation accuracy against test result. In this study, HIC target values in CAE were determined as 607 and 911 based on past developments. In addition, assignment of target values for each validation point were assumed to acquire over 65% score of Euro-NCAP pedestrian test [table 3]. Impactor stroke was measured by 50 degree direction which is approach angle.

Validation-process If 9 validation points are validated by all 15 design variables, calculation will take an enormous amount of time. Therefore, the authors took 3 validation steps as below. At first, worst validation point was determined after investigating severe validation point using 30 uniform random designs. Secondly, Optimization CAE was performed for the worst validation point so that stroke can minimize while satisfying target HIC. Lastly, performance of whole hood was confirmed whether the optimized shape improves other validation point performance.

Step1: Selection of worst validation point using 30 design variables.

Step2: Optimization for impactor stroke for worst validation point.

Step3: Confirmation all validation points with optimized shape.

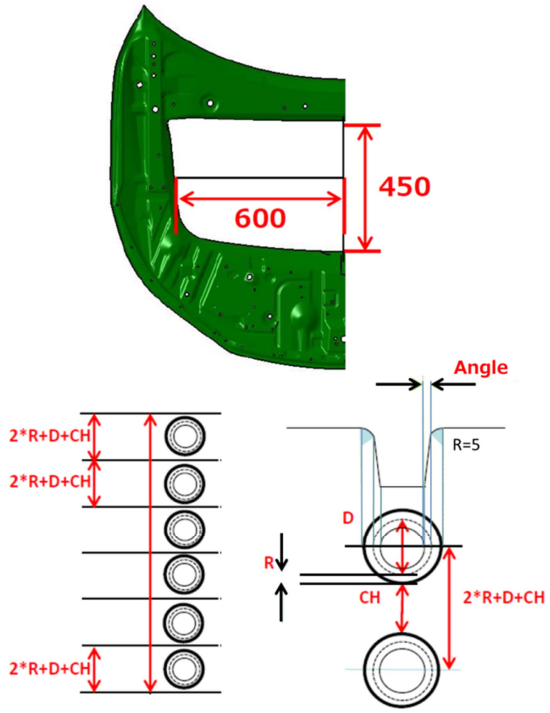

Figure 8. Relationship between arithmetic expression and emboss shape (Row)

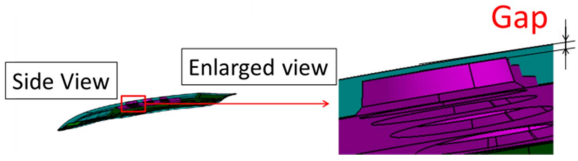

Figure 9. Gap between hood skin and frame

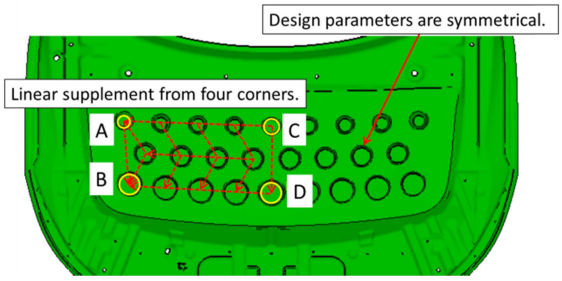

Figure .10 4angles and diameters of corner emboss

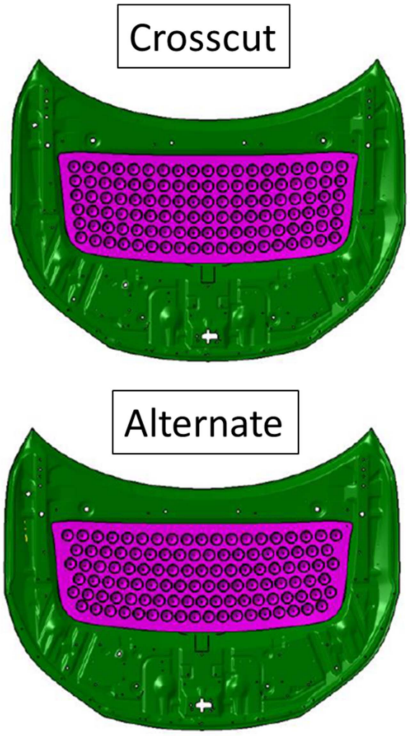

Figure .11 Array pattern of emboss

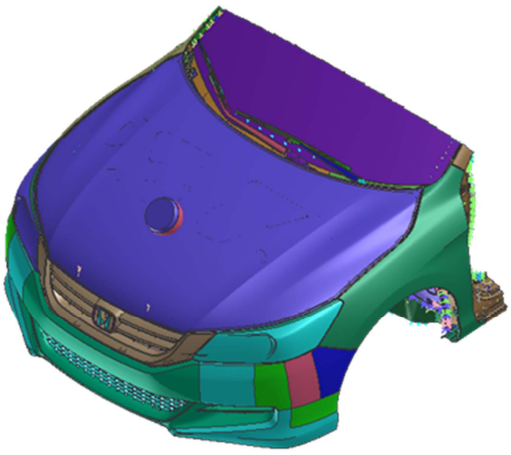

Figure .12 Vehicle model for optimization CAE

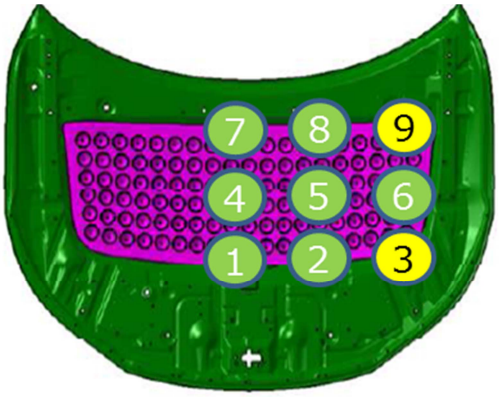

Figure .13 Validation point on emboss hood

Table 3.
Target value of HIC

Validation Point	Target HIC
1	607
2	607
3	911
4	607
5	607
6	607
7	607
8	607
9	911

RESULTS

Selection of worst validation point

Figure 14 shows that the relationship between HIC and stroke on each validation point by 30 uniform random designs within the design variables range determined at Table 2. This figure indicates that No6 is the worst validation point of them all. As a result, No6 was selected as the worst validation point.

Optimization for impactor stroke on worst validation point

Optimization condition was determined as below for the selected worst validation point. There are various algorithms for optimization. As this study has many design variables to search in large design space simulated annealing for global optimization was used.

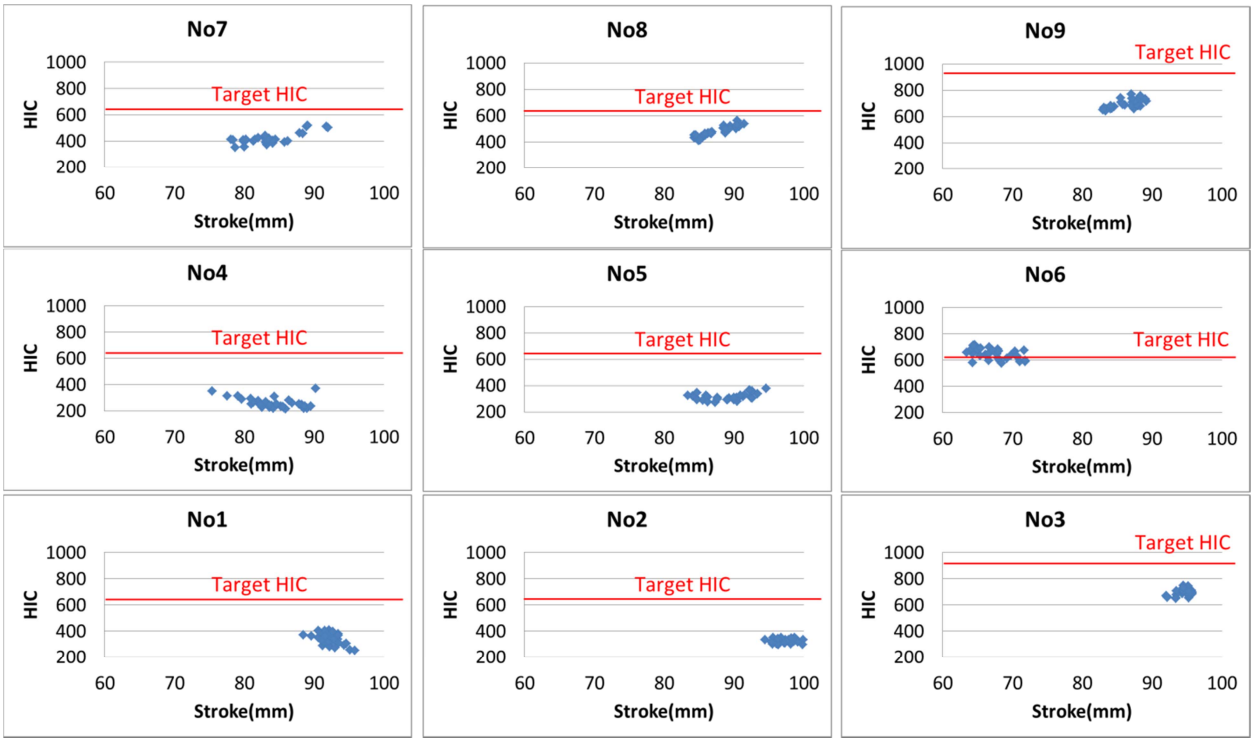

Figure 14. Relation between HIC and stroke on each validation point

Output variable: HIC, Impactor stroke

Objective function: Minimize impactor stroke

Boundary condition: Under HIC607

DOE (Design of Experiment) sampling: 30 designs by uniform random number

Optimizer: MOSA (Multi-Objective Simulated Annealing)

Total design numbers: 441

Figure 15 shows optimization calculation results on No6 validation point. The design which is in most lower left is the best solution in the figure.

Confirmation all points with optimized shape

Optimized shape on No6 was calculated for other validation point. However, HIC of No2 was over 607 [Table 4]. Therefore, the pareto solutions of No6 was investigated whether they can satisfy target HIC of No2 [Figure 16]. As a result, there were 3 solutions with HIC under 607 [Figure 17]. The shortest solution of stroke in the 3 solution was validated for other 7 validation points without No2 and No6. Then the optimized shape for No6 and No2 satisfied all HIC target. Furthermore, the authors compared the optimized shape with conventional hood shown at Figure 5 about HIC and stroke. Consequently, the crash stroke was reduced an average of 6% while satisfying target HIC for all validation points [Figure 18, 19][Table 6,7]. Figure 19 shows optimized shape.

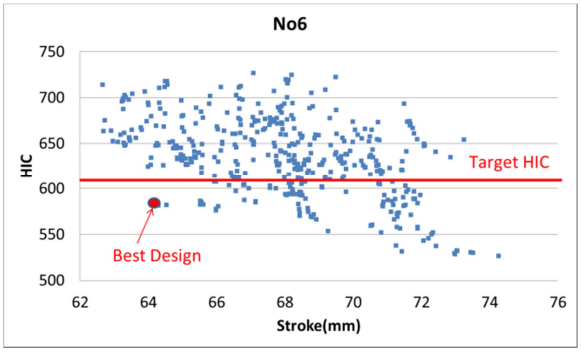

Figure 15. Optimization calculation results on No6 validation point

Table 4.
Results of HIC by No6 best design

	Target HIC	No6 best
HIC_1	607	524
HIC_2	607	**641**
HIC_3	911	753
HIC_4	607	317
HIC_5	607	408
HIC_6	607	582
HIC_7	607	452
HIC_8	607	498
HIC_9	911	789

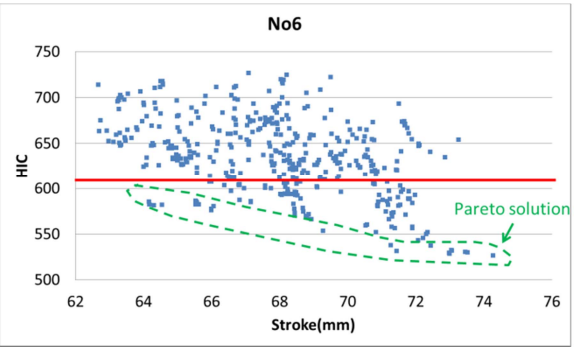

Figure 16. Pareto solution in optimized result

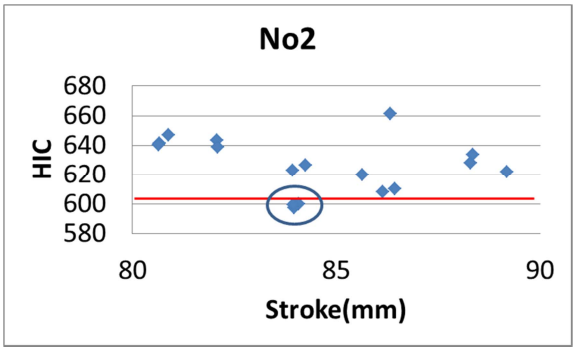

Figure 17. No2 CAE results using No6 pareto solution

Table 5.
Results of HIC by No6 pareto design

	Target HIC	No6 pareto
HIC_1	607	487
HIC_2	607	600
HIC_3	911	660
HIC_4	607	275
HIC_5	607	496
HIC_6	607	566
HIC_7	607	435
HIC_8	607	486
HIC_9	911	771

Table 6.
Comparison with conventional hood and optimized hood result (HIC)

	Target HIC	Conventional	No6 best	No6 pareto
HIC_1	607	456	524	487
HIC_2	607	389	641	600
HIC_3	911	809	753	660
HIC_4	607	384	317	275
HIC_5	607	525	408	496
HIC_6	607	748	582	566
HIC_7	607	621	452	435
HIC_8	607	653	498	486
HIC_9	911	777	789	771

Table 7.
Comparison with conventional hood and optimized hood result (Stroke)

	Conventional	No6 best	No6 pareto	Reduction rate
DISP_1	91	84	87	5%
DISP_2	92	81	84	9%
DISP_3	88	74	76	16%
DISP_4	80	75	80	1%
DISP_5	77	73	79	-2%
DISP_6	77	64	69	12%
DISP_7	80	75	79	1%
DISP_8	84	74	79	7%
DISP_9	77	65	70	10%
Ave	82.9	73.7	78	**6%**

Unit:mm

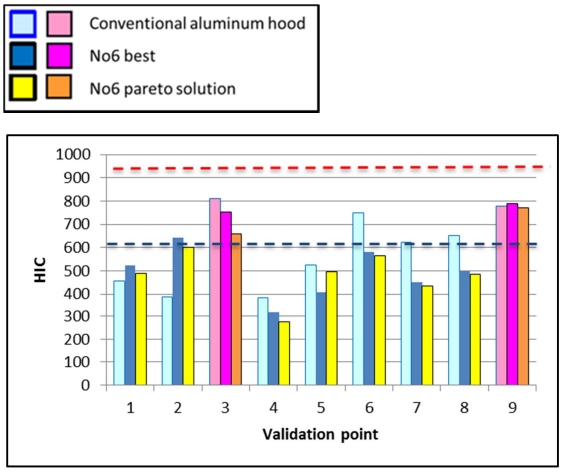

Figure 18. Comparison with conventional hood and optimized hood result (HIC)

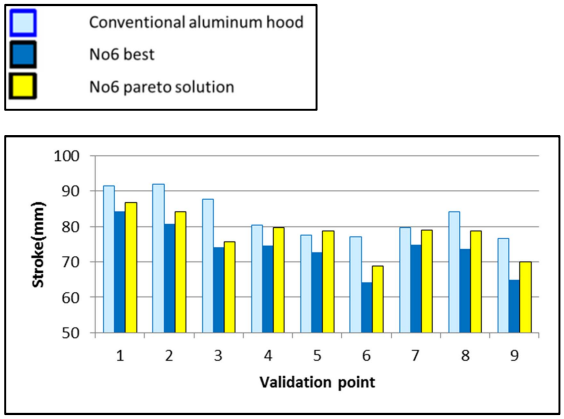

Figure 19. Comparison with conventional hood and optimized hood result (Stroke)

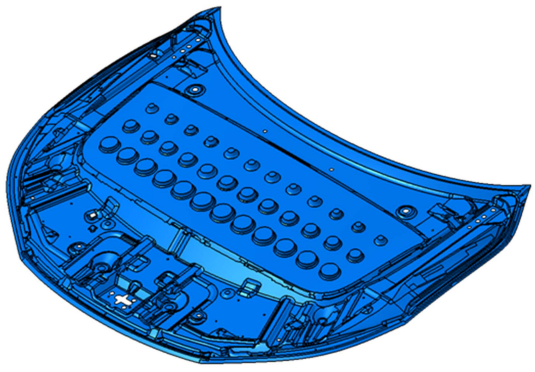

Figure 19. Optimized hood structure

DISCUSSION

Stroke effect analysis

Contribution analysis of acquired optimized solution was investigated. SS-ANOVA (Smoothing-Spline Analysis of Variance) was used for contribution analysis. This method mainly decomposes overall fluctuation into each one for every factor, and calculates each ratio between overall fluctuation and each one for every factor. Then Smoothing-Spline method is used for the decomposition [6]. Figure 20 shows that the frame thickness, skin thickness and gap of hood have contribution for stroke. Furthermore, effect size was investigated using Student-Chart within each design variable [Figure 21]. The effect size is plotted on the Y axis and it shows the strength of the relationship between the input and the output variable. A positive effect size value indicates a direct relationship with the output variable, whereas a negative value indicates an inverse relationship. This method resolves into upper and lower levels for each variable. The effect size is computed as the difference between mean of lower level and mean of upper level. In this way, it generates an ordered list of factors based on importance [7]. Figure 21 shows that frame thickness, the skin thickness and gap of hood has large effective size the same as SS-ANOVA. In addition, the vertical emboss number (NH), angle_A and angle_C have also effect. From these graph, it may be considered that these variables affect the stroke by varying hood stiffness.

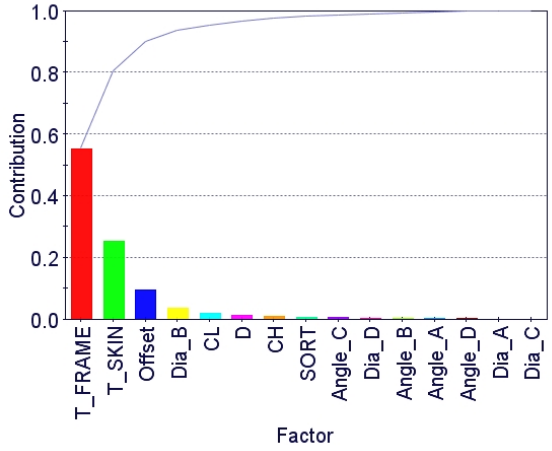

Figure 20. Contribution of stroke

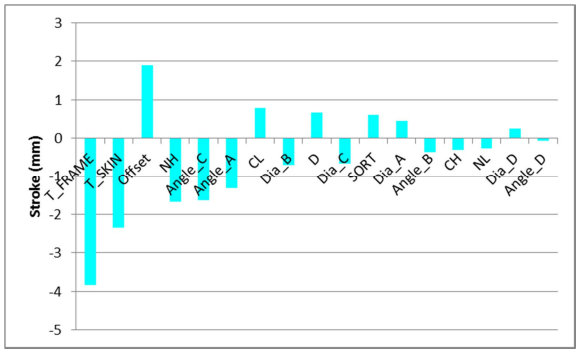

Figure 21. Student-Chart of stroke

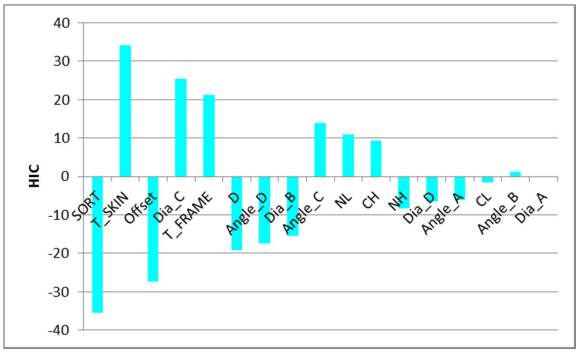

Figure 23. Student-Chart of HIC

HIC effect Analysis

The authors analyzed the HIC contribution as well as stroke. Figure 22 shows that the skin thickness, array pattern and gap of hood have large contribution from SS-ANOVA. Then the effect size was also analyzed by Student-Chart. Figure 23 shows that the skin thickness, array pattern and gap of hood have large effect size as same as SS-ANOVA. In addition, the emboss diameter and frame thickness also has an effect. On the other hand, the array pattern had contribution to HIC and not stroke. When the array pattern is changed, it may be thought that attitude of the initial G changes.

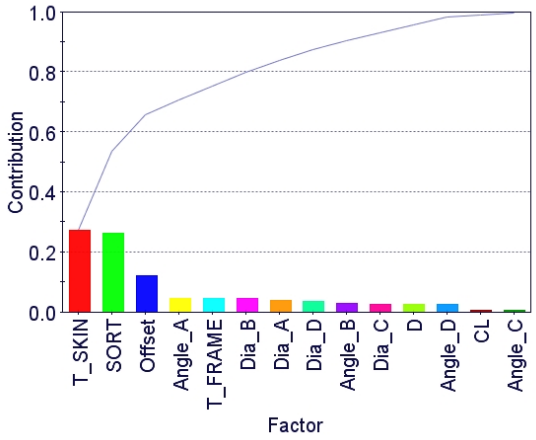

Figure 22. Contribution of HIC

Kinematics Analysis

Mechanical behavior of the optimized hood was analyzed on the No6 validation point. Then it was compared with how the kinematics changed from conventional hood. Figure 24 shows the waveform comparison of the conventional hood and optimized hood. It indicates that the initial and the latter G are closer to the ideal waveform rather than conventional hood. In addition, the strain energy distribution was compared at 2msec [Figure 25, 26]. It is thought that the initial G of optimized hood was improved by the increase in effective mass because the strain energy distribution area was large. Furthermore, the deformation kinematics at hood rear end was confirmed at the latter time. Because the conventional hood has shorter between the hood rear wall end and the cowl top which is supporting point, the hood deformation was interfered [Figure 27]. On the other hand, as the optimized hood was smoothing surface from the cowl top to emboss, the hood deformation was not interfered [Figure 28]. It became appropriate shape so that the latter G could decrease by geometry-based optimization.

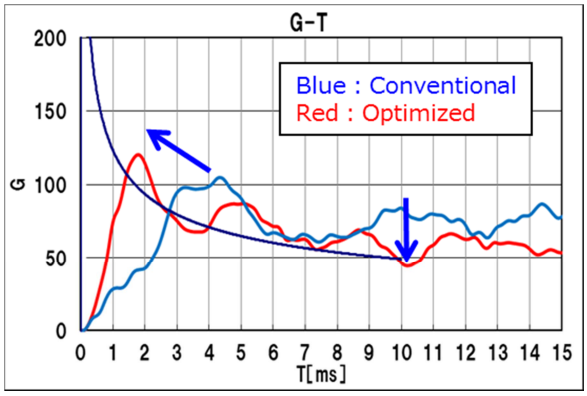

Figure 24. Waveform comparison of conventional hood and optimization hood

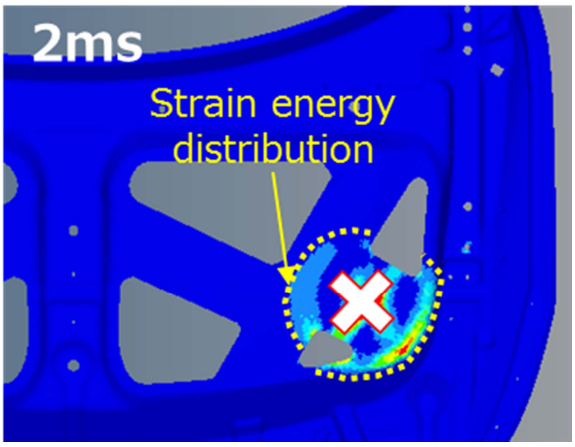

Figure 25. Strain energy distribution at the time of 2msec of conventional hood

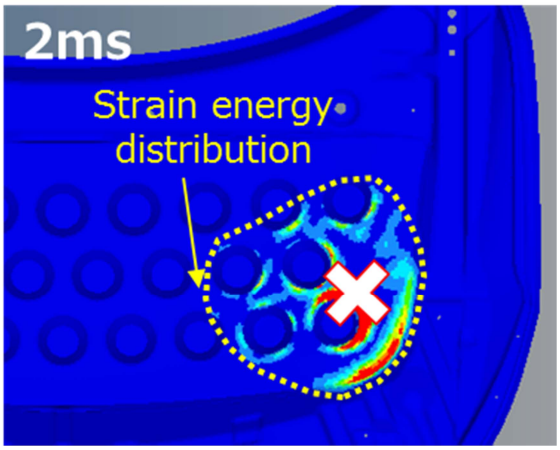

Figure 26. Strain energy distribution at the time of 2msec of optimized hood

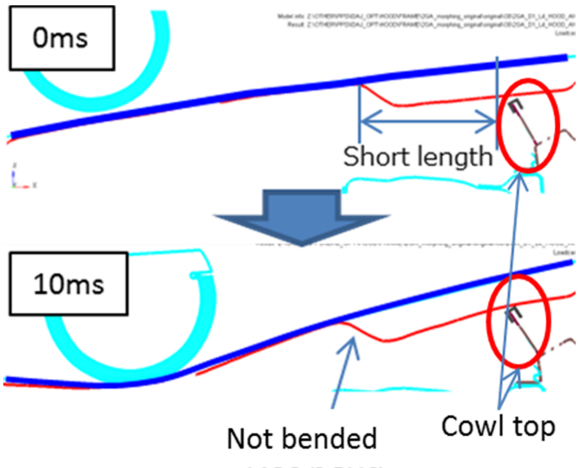

Figure 27. Conventional hood deformation between 0msec and 10msec

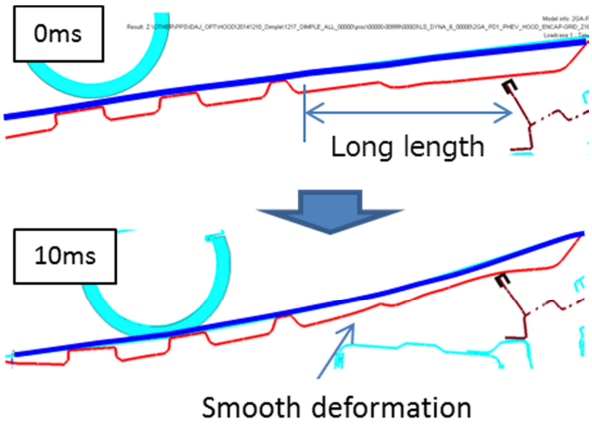

Figure 28. Optimized hood deformation between 0msec and 10msec

LIMITATION

In order to apply this research to vehicle development, it is necessary to review the stamping manufacturability of aluminum and to re-set design variable as probable realistic range.

CONCLUSIONS

The authors researched emboss aluminum hood structures which could help both lower HIC values and reduced stroke using geometry based optimization CAE.

The embossed hood reduced crash stroke 6% conserving target HIC as compared with conventional hood.

The design variables which have influence for stroke were frame thickness, skin thickness and gap of hood frame and skin.

The design variables which have influence for HIC were skin thickness, array pattern and gap of hood frame and skin.

The initial and the latter G of the optimized hood come close to ideal waveform.

Time which optimized calculation took is about five days in this research. Since design period is restricted in development short optimization computation time is desirable. In this research, design variables which affect contribution and effect size became clear. In that case optimization computation time can be short by fixing design variable which does not contribute application to vehicle development can be realized.

REFERENCES

[1] Transportation statistics, the National Police Agency, 2016 (in Japanese)

[2] Global technical regulation No. 9 PEDESTRIAN SAFETY

[3] Development of Aluminum Hood Structure for Pedestrian Protection, Koki Ikeda et_al., SAE 2003-01-2793, 2003

[4] Geometry Based Topology Optimization - Improving Head Impact Performance of an Engine Hood, D.Weiss et_al., 7th European LS-DYNA Conference, 2009

[5] Concept of Hood Design for Possible Reduction in Pedestrian Head Injury, Yutaka Okamoto et_al., 13th ESV, Paper No 94-S7-W-14, 1994

[6] C. Gu. Smoothing Spline ANOVA Models. Springer-Verlag, New York, 2002.

[7] modeFRONTEIR user guide –Student Chart-, ESTECO, 2016